

Advanced Treatment: Tackling Paracetamol with Fenton Oxidation and Membrane Hybrid Processes

Fadhila Malahayati Kamal, Sucipta Laksono*, Sandyanto Adityosulindro

Department of Civil and Environmental Engineering, Faculty of Engineering, Universitas Indonesia, Depok, INDONESIA

*Corresponding author: sucipta.laksono04@ui.ac.id

SUBMITTED 25 April 2024 REVISED 5 June 2024 ACCEPTED 25 June 2024

ABSTRACT Paracetamol (PCT) in aquatic environments has become a global concern due to its potential harm to humans and environments. However, conventional water treatment was only able to degrade PCT partially. It was necessary to treat PCT contaminated water with tertiary technologies in particular by combination approach, such as Fenton oxidation and membrane filtration process. This combined approach enabling mitigation of large chemical footprint and iron residue associated with Fenton oxidation, as well as reducing fouling tendency of the membrane. The aim of this study was to evaluate the PCT removal efficiency by hybrid technology Fenton oxidation and membrane filtration. The membrane performance during the filtration process was also analyzed. As an important parameter for Fenton process, concentration of H_2O_2/Fe^{2+} with ratio of 1:0.5 resulted in optimal removal of 45% PCT in terms of COD removal. However, separation using flat sheet Polyethersulfone Ultrafiltration (UF) with constant flux of $120 L/m^2 \cdot h$ resulted in insignificant of COD removal. Nevertheless, the UF process was able to remove up to 54% of Fe^{2+} at pH in alkaline condition with 8.5. In addition, a decrease in membrane permeability down to $0.2 L/m^2 \cdot h / bar$ over time, according to the filtered specific volume during the UF process, indicates fouling of the UF membrane during the 120 minutes of filtration. While the combined approach does not show significant improvement in COD removal, it does help to reduce the chemical footprint of the process, which is an important factor for the applicability of the selected water treatment method.

KEYWORDS Fenton, Hybrid Process, Iron, Membrane Filtration, Paracetamol

© The Author(s) 2024. This article is distributed under a Creative Commons Attribution-ShareAlike 4.0 International license.

1 INTRODUCTION

Recently, contaminated water by medical substance happened due to detection of traces paracetamol (PCT) in Jakarta Bay area. PCT substances was detected at two locations with $610 ng L^{-1}$ in Angke and $420 ng L^{-1}$ in Ancol, respectively (Koagouw et al., 2021). In general, contaminated surface water by PCT across aqueous matrices was found around the world. However, this phenomenon was occurred first time in Indonesia. A comparison from various countries, China and America were detected the highest concentration of PCT in their wastewater. As for surface water, its concentration was also found various in Asia, Europe, and America with a concentration range of $9.8 ng L^{-1}$ to $300 \mu g L^{-1}$ (Phong Vo et al., 2019). Despite the low concentrations observed, the detection of PCT on surface water matrices raised concerns regarding its potential negative impacts on human health and organisms. The presence of PCT had a potential cause for damaging genetic code, lipid oxidation degradation, and protein denaturation in cells. The toxicological profile of PCT ranging from minimal to moderate in severity, depending on its dosage and time of exposure (Phong Vo et al., 2019).

Exhibiting a similar characteristic like other pharmaceutical pollutants, PCT's only can be partially removed by conventional water treatment technologies with ef-

ficiencies as low as 10% (Alessandretti et al., 2021; Husain Khan et al., 2023). The limitations of conventional water treatment explained the necessary for tertiary water treatment process to increase PCT removal efficiency in across water matrices. Related to the basic principle, the application of membrane technology has become a promising technology and found in commercial as an alternative to flocculation, purification techniques, adsorption, and distillation. Furthermore, membrane operation was considered as a flexible process that can be applied to treat various water matrices, including industrial wastewater. As additional advantage, application of membranes was considered to be simple and requires relatively low energy in particularly by employing ultrafiltration membrane. Despite promising, the disadvantage of this process is the tendency for fouling, which results in decreased membrane performance in water treatment (Rosman et al., 2018).

Alongside membrane technology, Advance Oxidation Processes (AOPs) have become one of the alternative treatment options for pharmaceutical residue. AOPs rely on the production of hydroxyl radicals to degrade refractory contaminants, e.g. pharmaceuticals that cannot be degrade fully by conventional processes. Hence, AOPs is suitable for PCT removal treatment

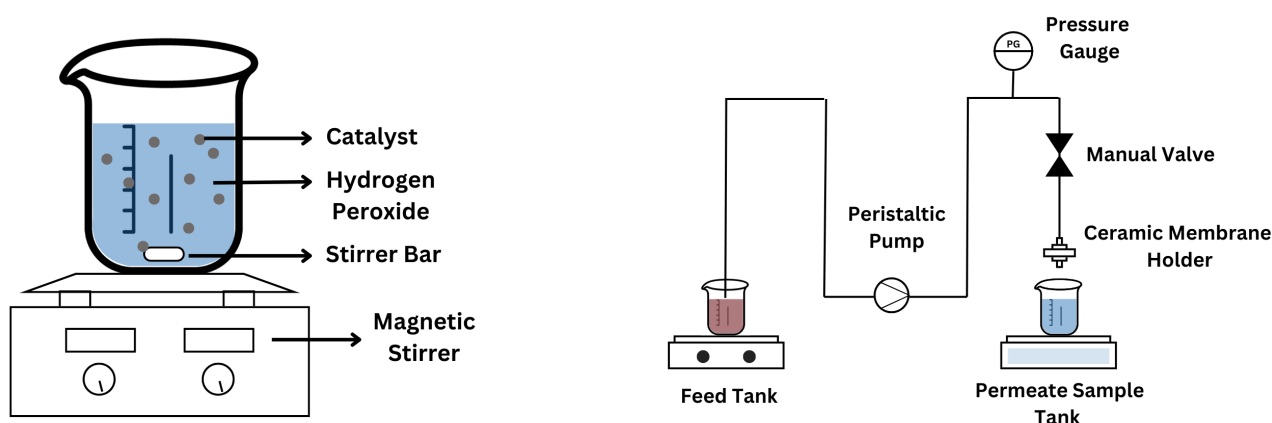


Figure 1 Experimental Setup

from across water matrices. One promising AOPs technology is Fenton oxidation, which utilize iron as catalyst and hydrogen peroxide to accelerate the formation of hydroxyl radicals (Ziembowicz and Kida, 2022). Fenton oxidation shows a broad spectrum of effectiveness in treating pharmaceuticals, sensitive to various operational factors such as pH, pollutant concentration, type and dosage of catalyst and other parameters. (Mirzaei et al., 2017). Therefore, study showed that Fenton efficiency ranged from 35% to 99% in treating pharmaceuticals substances (Ganiyu et al., 2015). On the other hand, Fenton process has significant chemical footprint and the potential for residual contamination of iron residue, requiring downstream water treatment (Ziembowicz and Kida, 2022).

Integrating Fenton oxidation and membrane filtration overcomes their individual limitations, paving the way for a high-performance PCT treatment solution. Fenton oxidation, placed as the initial treatment to degrades the target pollutant, breaking down the complex molecules into simpler and harmless molecules. Followed by membrane separation as the processing unit to remove simple molecules. Therefore, installation of Fenton as a pre-treatment for membrane process provides better advantages such as minimize fouling and prolong membrane performance during the separation process. For the main advantages, the membrane can retain unoxidized pollutants and resulted better water quality. This provides a flexible system in which the by-products produced can be further oxidized by immobilizing the catalyst which later can be separated by the filtration process (Rosman et al., 2018). Therefore, this study aims to evaluate the PCT removal efficiency in terms of COD removal by hybrid technology combining Fenton oxidation and membrane filtration as well as the membrane performance during the filtration process.

2 METHODS

PCT solutions were prepared by dissolving predetermined amount of PCT in distilled water, where the PCT used in this study had a purity of more than 98%. For Fenton experiment, H_2O_2 30% w/w and $\text{FeSO}_4 \cdot 7\text{H}_2\text{O}$ was employed as reagent. Furthermore, the pH of the PCT solution was purposely adjusted to 3 using a H_2SO_4 1M. For membrane experiment, flat sheet Polyether-sulfone (PES) membranes with an average molecular weight cut-off of 30 nm and a diameter of 47 mm (surface area= 1,735.64 mm^2), purchased from Sterlitech Corporation, were used for the ultrafiltration (UF) experiments. After the filtration process, the fouled PES membrane was characterized through SEM images and FTIR analysis to identify the influence of the filtration process on the membrane's properties. All experiments were conducted at laboratory scale in batch mode, with each experiment replicated twice.

Fenton experiments employed a 1000 mL reactor containing 500 mL of 100 mg L^{-1} PCT solution (Figure 1). In the reactor, a constant ratio of COD/ H_2O_2 1:1 was also maintained. Furthermore, H_2SO_4 1M was added to adjust the solution's pH into 3 followed by additional various dosages of $\text{FeSO}_4 \cdot 7\text{H}_2\text{O}$ based on $\text{H}_2\text{O}_2/\text{Fe}^{2+}$ ratio. Moreover, a magnetic stirrer agitated at 150 rpm at room temperature for 60 minutes was placed in the reactor media. As an analytic parameter, COD was measured as an indicator for PCT's presence. Additionally, iron residues were measured and collected after the one hour of Fenton process. Thereafter, the effluent from the Fenton process (Figure 1) was filtered through UF membrane at a constant flux of 120 $\text{L m}^{-2} \text{h}^{-1}$ and the filtration was achieved by using a peristaltic pump (Longer pump type BT300-2J) at a flow rate of 2 rpm. Subsequently, the membrane permeates were also collected to test for COD and iron residue. Subsequently, NaOH 1M was also used as a pH adjustor on later exper-

iment of iron residual removal.

PCT removal in Fenton oxidation was assessed by comparing COD concentration after the addition of H_2O_2 and after the 60 minutes of oxidation. Conversely, for UF process, the removal was determined by comparing COD in the feed solution with the membrane permeate. This was measured through Equation 1, where R is membrane retention, C_p is substance concentration in the permeate stream and C_f is substance concentration in the feed.

$$R = 1 - \frac{C_p}{C_f} \quad (1)$$

UF membrane performance was assisted by observing the changes in membrane's permeability to the permeate volume. Accordingly, every 5 minutes the pressure readings and filtrate volume were recorded to identify membrane flux and transmembrane pressure. Thereafter, membrane permeability measured through Equation 2, where W is membrane permeability ($L m^{-2} h^{-1} .bar$), J is water flux ($L m^{-2} h^{-1}$), and ΔP is transmembrane pressure (bar).

$$W = \frac{J}{P} \quad (2)$$

As for J, water flux ($L m^{-2} h^{-1}$), is identified by Equation 3. Q is filtered water flow ($L h^{-1}$), and A is the surface area of the membrane (m^2). Consequently, V_{sp} filtered specific volume ($L m^{-2}$) was identified through Equation 4, where V_p is permeate volume (L) and A is membrane surface area (m^2).

$$J = \frac{Q}{A} \quad (3)$$

$$V_{sp} = \frac{V_p}{A} \quad (4)$$

3 RESULTS

In this section, hybrid processes for PCT treatment were evaluated through Fenton oxidation and membrane filtration perspective.

3.1 Effect of H_2O_2/Fe^{2+} ratios

The assessment of Fenton oxidation to treat PCT was done through various $FeSO_4.7H_2O$ dosages obtained through H_2O_2/Fe^{2+} ratios. Ranging from 1:0.33 to 1:3, the amounts iron added were equivalent to 66-396 mg/L of Fe^{2+} . The results shown in figure 2, revealed

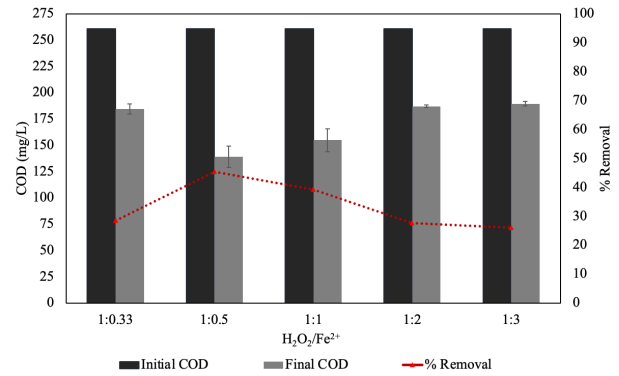


Figure 2 PCT's Removal (Represented in COD) From Fenton Oxidation

that each ratio resulted in a variety of PCT removal levels from the initial $100 mg L^{-1}$ PCT's COD plus the addition of $198 mg L^{-1} H_2O_2$ resulted in COD of $261 mg L^{-1}$. The lowest H_2O_2/Fe^{2+} ratio of 1:0.33, exhibited minimal PCT removal efficiency, achieving only 28%. However, at the highest ratio of H_2O_2/Fe^{2+} 1:3, did not result in a substantial improvement in PCT removal, unexpectedly 4% lower than the lowest ratio at 26% of PCT removal. On the other hand, Moderate efficiencies of 39% and 27% were observed at H_2O_2/Fe^{2+} ratios of 1:1 and 1:2, respectively. In contrast, the optimal removal of 45% was observed at the ratio of 1:0.5. Consequently, the increase of catalyst dosage did not increase removal efficiency proportionally.

3.2 Membrane Performance

The UF performance was assisted by its efficiency to remove PCT and iron residue, and its operation performance.

3.2.1 UF for PCT Removal

Figure 3 shows the results of the UF permeate. Due to the UF process feed being the effluent of the Fenton oxidation process (Figure 2), the initial COD values varied with each H_2O_2/Fe^{2+} ratio. Notably, at the lowest ratio (1:0.33), the permeate COD remained high at a $176 mg L^{-1}$, indicating only 4,6% removal by UF. This negligible COD removal was also observed at higher H_2O_2/Fe^{2+} . At the H_2O_2/Fe^{2+} ratios of 1:0.5; 1:1; 1:2; and 1:3 UF membrane only able to remove COD less than 5%, leading to the permeate COD concentration that closely resembled the initial feed COD concentration. These results demonstrated the lack of UF process contribution to PCT removal.

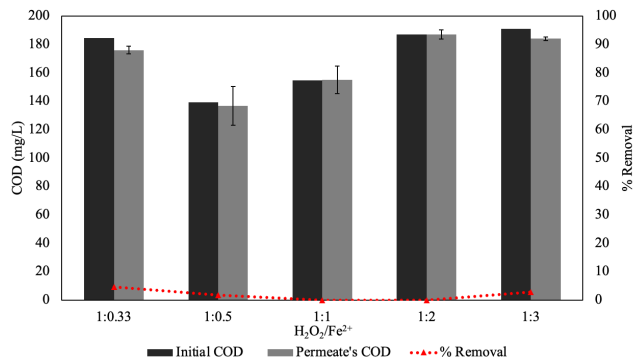


Figure 3 PCT's Removal (Represented in COD) at Various Catalyst Dosages from UF

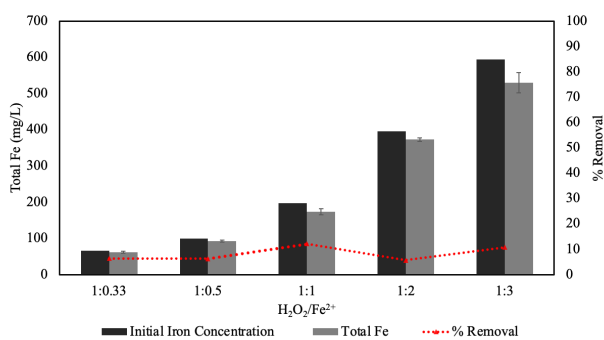


Figure 4 UF to Remove Iron Residue

3.2.2 UF for Iron Residue Removal

UF performance was also assisted through the efficiency of the filtration process to remove iron residue, from Fenton's catalyst at pH 3. As shown in figure 4, the permeate's iron residue concentrations were proportional to the feed's iron concentrations. For all the H_2O_2/Fe^{2+} ratios (1:0.33; 1:0.5; 1:1; 1:2 and 1:3) UF showed a removal rate subject to a 15% threshold. Similarly, to the UF performance in removing PCT, UF also demonstrated the lack of contributions to remove iron residue. This results in iron concentrations in the permeates ranging from 61 mg L^{-1} to 530 mg L^{-1} .

Following the previous findings of the insignificant role of UF to treat iron residue, series of experiments of adjusted membrane's feed pH were conducted. The experiments were done using the catalyst ratio of 1:0.5, the optimal ratio yielded from Fenton oxidation process. The initial feed's pH was adjusted to pH 3; 5; 6.5; and 8.5 through the addition of NaOH 1M. As shown in Figure 5, a direct correlation was observed between feed solution pH and iron removal efficiency through UF. At pH 3, the removal efficiency was demonstrably low, achieving less than 10%. Conversely, increasing the feed solution pH to 5 and 6.5 resulted in improved removal efficiencies of 33% and 38.1%, respectively. The highest removal efficiency of 58.1% was achieved at a

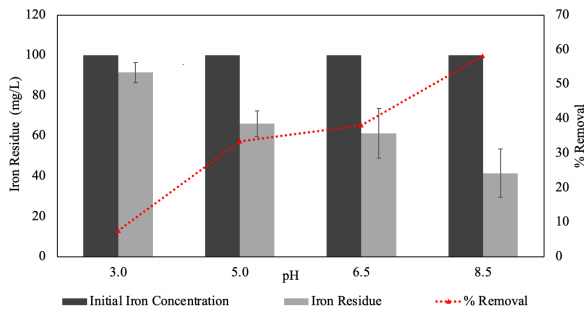
feed solution pH of 8.5.

3.2.3 Filtration Cycle

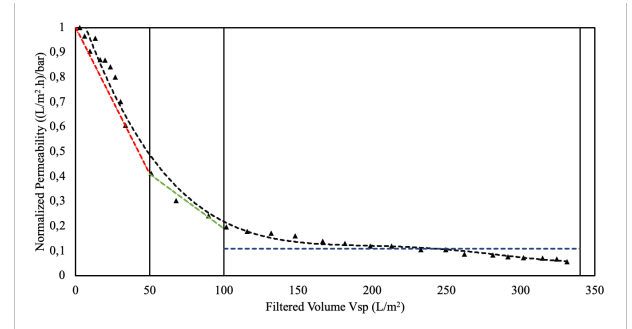
Membrane performance was able to be evaluated through the filtration curve by comparing the normalization of membrane's permeability decline with the specific filtered volume (V_{sp}) during the 120 minutes of filtration (Figure 5). As shown from figure 55 in general, the UF permeability decreased as the filtration of water increased. Furthermore, in order to understand the performance, membrane filtration curve could be observed by divided the performance curve into several section (Abdelrasoul et al., 2013). Despite decreasing over filtration time, different decline of membrane performance was found. It could be seen at the early stages a steep membrane permeability decline was observed Figure 5 (region (I)) with the decrease of membrane permeability of $0,6 \text{ (L m}^{-2} \cdot \text{h}^{-1})/\text{bar}$ at specific filtered volume of 50 L m^{-2} . Furthermore, at a second stage (Figure 5 region (II)), a less steep membrane permeability declines of $0,2 \text{ (L m}^{-2} \cdot \text{h}^{-1})/\text{bar}$ was occurred during filtration process at specific filtered volume between $50 - 100 \text{ L m}^{-2}$. In the later stages ((Figure 5 region (III)) of filtration between filtered specific volume of $100 - 340 \text{ L m}^{-2}$, the linier membrane permeability decreases of $0,15 \text{ (L m}^{-2} \cdot \text{h}^{-1})/\text{bar}$ was revealed. Although comparable membrane permeability declines between the later stages and second stages was found, the filtered specific volume was found to be different with 240 L m^{-2} and 50 L m^{-2} , respectively. Therefore, the less filtered specific volume represented a severe membrane fouling.

3.3 Membrane Characterization

Membrane characterization was done through SEM images to identify the surface characteristic of the membrane and FTIR to identify the functional groups and chemical species of the membranes. As shown in figure 6b, SEM images of used UF membrane displays particle accumulation than the pristine membrane (Figure 6a). Based on the scale provided in the SEM images (Figure 6b), the particles covering the membrane surface exhibit a wide range of sizes, as exemplified by the particles circled in red. It was estimated that the smallest particles occluding the membrane pores have a size of $0.167 \mu\text{m}$, the upper particle also circle in measures $0.32 \mu\text{m}$ and the largest measures $2.67 \mu\text{m}$. These particles can be retained on the membrane and detected during characterization due to size exclusion mechanisms, where the particle size far exceeds the membrane pore size of 30 nm . As for the FTIR results (Figure 6c and Figure 6d), showed wavelength peaks ranging from 3385 cm^{-1} to 551 cm^{-1} . Pristine membrane FTIR result (Figure 6c) showed prominent wavelength peaks at 3362.18 cm^{-1} ; 1638.53 cm^{-1} ; 1485.27 cm^{-1} ; and 1148.52 cm^{-1} . Similarly, the FTIR result for used



(a) UF to Remove Iron Residue at Adjusted pH



(b) Filtration Cycle

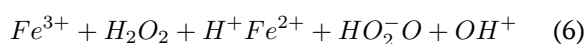
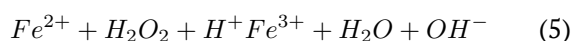
Figure 5 Figures demonstrating UF to Remove Iron Residue and Filtration Cycle

membrane (Figure 6d) did not show significant wavelength difference from pristine membrane. The used membrane showed wavelength peaks at 3385.50 cm^{-1} ; 1638.82 cm^{-1} ; 1484.61 cm^{-1} ; and 1146.85 cm^{-1} . However, the intensity of the functional group peaks (Y-axis) in the spectrum of the used membrane (Figure 6d) exhibits a slight increase. Compared to the pristine membrane (Figure 6b), the intensity has risen by approximately 10%. This suggests a foulant layer might be present on the surface of the membrane.

4 DISCUSSIONS

4.1 Fenton Oxidation

Analysis of the Fenton experiment data indicates that the dosage of catalyst had a significant effect on the removal of PCT (Figure 2). In agreement with the result of this study, a previous study done by (Van et al., 2020) also showed that at the $\text{FeSO}_4 \cdot 7\text{H}_2\text{O}$ dosage of 100 mg L^{-1} and H_2O_2 200 mg L^{-1} ($\text{H}_2\text{O}_2/\text{Fe}^{2+}$ 1:0.5) resulted in the optimal COD removal of PCT. This phenomenon was caused by the presence of hydroxyl radicals that react with the compound PCT. This non-selective oxidation breaks down these molecules into simpler intermediates products resulting in the generation of some derivatives and carboxylic acids and continue the process until the organic compounds are entirely mineralized to water and carbon dioxide (Sychev and Isak, 1995; Adityosulindro et al., 2018; Pacheco-Álvarez et al., 2022). The reaction formed through equation 5 and 6



While the addition of Fe^{2+} theoretically enhances hydroxyl radical formation, excess Fe^{2+} leads to the hydroxyl radical scavenging. This is where these reactive

species of oxygen reacted with the excess Fe^{2+} resulting in less reactive oxygen species (Van et al., 2020). Therefore, at the $\text{H}_2\text{O}_2/\text{Fe}^{2+}$ ratio of 1:0.5 was the optimum ratio to generate hydroxyl radicals to break down PCT compound.

4.2 Membrane Filtration

4.2.1 PCT Removal

The UF performance, as shown in Figure 3, exhibited negligible retention of PCT across all catalyst variations. This limited removal efficiency stems from the PES 30 nm membrane's pore size (600 kDa) being significantly larger than the target molecule, PCT (0.1-0.3 kDa), hindering size-based separation. These results align with prior research concluding the ineffectiveness of UF membranes for PCT removal. This study confirms these findings with a measured rejection range of 3-9%, further highlighting the limitations of this approach for this specific pollutant.

In addition to the size exclusion mechanism, the limited rejection of PCT by UF membrane can be attributed to adsorption onto the membrane surface, influenced by the octanol/water partition coefficient (Log Kow) of the pollutant. PCT has a low value of Log Kow, 0.46, signifies its strong hydrophilic nature (Islam et al., 2024). This condition results in minimal adsorption onto the membrane and contributing to the low COD rejection (Ganiyu et al., 2015).

4.2.2 Iron Removal

UF performance, evaluated through the iron removal also showed the inability of the UF process to remove the Fenton catalyst (Figure 4). Inevitably, this phenomenon was also caused by the size exclusion mechanism of the membrane to retain pollutant. During Fenton oxidation, iron catalyst transformed into dissolved iron, characterized by an estimated size of 1 nm

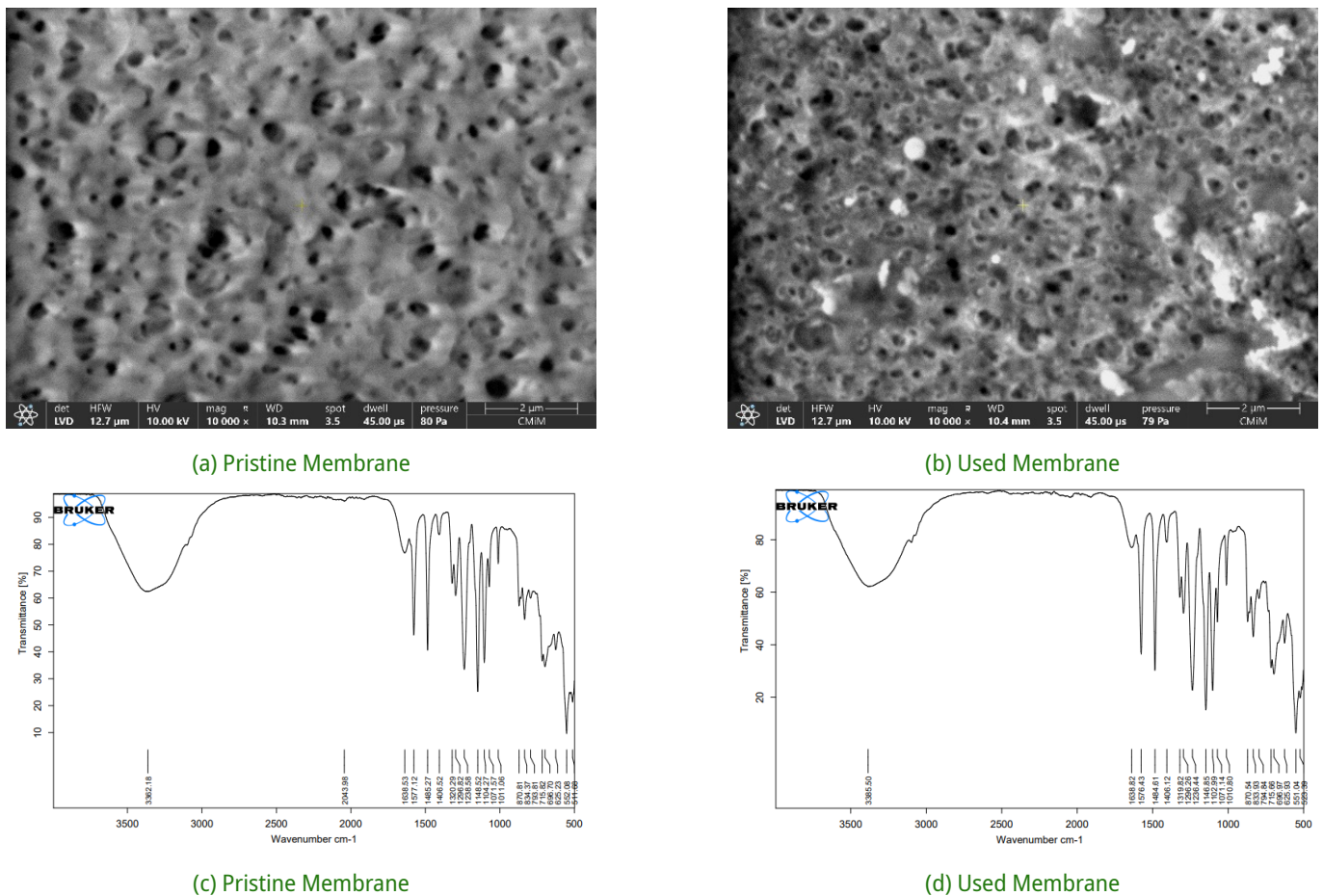


Figure 6 Membrane Characterization: 1 SEM Images. 2 FTIR

(Li et al., 2022; Pacheco-Álvarez et al., 2022). Hence, the larger membrane pore size (30 nm) unable to retain the dissolved catalyst. However, when the pH was adjusted to 8.5, UF was able to retain the iron catalyst up to 58% (Figure 5). As pH increases, Fe^{2+} undergoes rapid oxidation, forming microscopic Fe^{3+} particles. These particles agglomerate over time by merging with one another, concurrently releasing hydrogen ions. The growing particles attract more Fe^{2+} , forming ferrihydrite flocs. These flocs are responsible for the larger particle sizes observed early in the reaction. Higher pH allows faster transformation of Fe^{2+} to Fe^{3+} , leading to faster particle formation and complete oxidation (Hove et al., 2008).

4.2.3 Filtration Cycle

Membrane Based on Figure 5, the membrane's permeability value demonstrates a progressive decrease as the filtered water volume accumulates. The foulant on the membrane surface obstruction manifests as increase flow resistance, observed in elevation in pressure which leads to decreased in permeability in order to keep a constant flux filtration system (Ahmed et al., 2023). Related to the fouling mechanisms, the early stages of filtration could be explained as a standard

blocking, a steep decline might occur due to internal blocking, likely originates from precipitated iron in the effluent of the Fenton oxidation process, after the pH is adjusted to 8.5 and the PCT particles. At the second stage, most of the foulants blocked internal and some of the substances were precipitated on membrane surface and indicate intermediate blocking phenomenon. At later stages, the substances were deposited on the surface and cake layer was formed. Furthermore, several studies revealed that the standard blocking was responsible for irreversible fouling and influenced for shorter lifespan of the membrane in real practical application (Abdelrasoul et al., 2013).

4.3 Membrane Characterization

SEM images provide detailed information about the surface morphology, shape, structure of the membrane material and foulants (Alqaheem and Alomair, 2020). Figure 6b depicts the visualized foulants, highlighting the formation of particles subsequent to the filtration process (Figure 6a). As mentioned in section 3.3, the detection of the foulant layer occurs because of the size exclusion mechanism where the foulant particle sized nearly 100 times the membrane pores. The occurrence of fouling is further supported by the FTIR results,

which show that the membrane has a slightly higher spectrum intensity after filtration, indicating an in concentration increase of the functional groups (Arahman et al., 2022). This finding provides supporting evidence that membrane permeability decreases due to the formation of a foulant layer on the membrane surface (Al-Sawaftah et al., 2021).

On the other hand, the FTIR result did not exhibit notable differences of the membrane before (6c) and after filtration (6d). Spectroscopic analysis revealed peaks at $3.362 - 3.385 \text{ cm}^{-1}$, consistent with N-H stretching vibrations. Furthermore, peaks observed at 1.638 cm^{-1} and 1.485 cm^{-1} were attributed to C=O and C-N stretching vibrations, respectively (Nandiyanto et al., 2019; Kuttiani Ali et al., 2021).

The disparity of both characterization methods is attributed to the analytical strengths of each technique. SEM excels at high-resolution imaging of surface morphology, enabling the detection of physical changes such as the presence of foulants. In contrast, FTIR primarily analyzes the bulk chemical composition of the material. While foulants may not significantly alter the overall chemical fingerprint of the membrane, they can nonetheless impact its performance and surface properties (MacKeown et al., 2022).

5 CONCLUSION

In conclusion, Fenton oxidation demonstrated efficacy in removing PCT in terms of COD reduction up to 45%. Conversely, the UF membrane process exhibited minimal impact on PCT owing to its size-exclusion mechanism. However, the UF process was effective to remove iron residue at an alkaline pH of 8.5 up to 58%. It's important to note that even with efficient iron residue removal, subsequent filtration analysis revealed the presence of fouling on the UF membrane. This fouling, identified by decreased membrane permeability and the presence of particulate matter on the membrane surface through characterization techniques, is likely caused by a standard blocking mechanism. Standard blocking occurs when iron species or other Fenton oxidation byproducts deposit within the membrane pores, reducing its efficiency over time and potentially shortening its lifespan.

This study proposes an alternative method for understanding and managing PCT pollutants, opening doors for further research. Fenton oxidation effectively degrades PCT in simulated PCT wastewater, but future studies might explore the underlying mechanisms in complex environments like industrial or hospital wastewater. Additionally, using High-Performance Liquid Chromatography (HPLC) techniques can improve the accuracy of PCT identification. While UF retains the iron catalyst during the process, exploring nanofiltration

or reverse osmosis in combination with Fenton oxidation might lead to even better PCT removal. Further research on byproduct toxicity, environmental impact, economic feasibility, and large-scale implementation is needed to solidify this process as a practical solution for sustainable PCT removal from various water sources.

DISCLAIMER

The authors declare no conflict of interest.

ACKNOWLEDGMENTS

This study was financially supported by Universitas Indonesia through PUTI 2023 research grant.

REFERENCES

- Abdelrasoul, A., Doan, H. and Lohi, A. (2013), Fouling in membrane filtration and remediation methods, in 'Mass Transfer - Advances in Sustainable Energy and Environment Oriented Numerical Modeling', InTech. URL: <https://doi.org/10.5772/52370>
- Adityosulindro, S., Julcour, C. and Barthe, L. (2018), 'Heterogeneous fenton oxidation using fe-zsm5 catalyst for removal of ibuprofen in wastewater', *Journal of Environmental Chemical Engineering* 6(5), 5920–5928. URL: <https://doi.org/10.1016/j.jece.2018.09.007>
- Ahmed, M., Amin, S. and Mohamed, A. (2023), 'Fouling in reverse osmosis membranes: monitoring, characterization, mitigation strategies and future directions', *Heliyon* 9(4), e14908. URL: <https://doi.org/10.1016/j.heliyon.2023.e14908>
- Alessandretti, I., Rigueto, C., Nazari, M., Rosseto, M. and Dettmer, A. (2021), 'Removal of diclofenac from wastewater: A comprehensive review of detection, characteristics and tertiary treatment techniques', *Journal of Environmental Chemical Engineering* 9(6), 106743. URL: <https://doi.org/10.1016/j.jece.2021.106743>
- Alqaheem, Y. and Alomair, A. (2020), 'Microscopy and spectroscopy techniques for characterization of polymeric membranes', *Membranes* 10(2), 33. URL: <https://doi.org/10.3390/membranes10020033>
- AlSawaftah, N., Abuwatfa, W., Darwish, N. and Hussein, G. (2021), 'A comprehensive review on membrane fouling: Mathematical modelling, prediction, diagnosis, and mitigation', *Water* 13(9), 1327. URL: <https://doi.org/10.3390/w13091327>
- Arahman, N., Jakfar, J., Dzulhijjah, W., Halimah, N., Silmina, S., Aulia, M., Fahrina, A. and Bilad, M. (2022), 'Hydrophilic antimicrobial polyethersulfone

membrane for removal of turbidity of well-water', *Water* **14**(22), 3769.

URL: <https://doi.org/10.3390/w14223769>

Ganiyu, S., van Hullebusch, E., Cretin, M., Esposito, G. and Oturan, M. (2015), 'Coupling of membrane filtration and advanced oxidation processes for removal of pharmaceutical residues: A critical review', *Separation and Purification Technology* **156**, 891–914.

URL: <https://doi.org/10.1016/j.seppur.2015.09.059>

Hove, M., van Hille, R. and Lewis, A. (2008), 'Mechanisms of formation of iron precipitates from ferrous solutions at high and low ph', *Chemical Engineering Science* **63**(6), 1626–1635.

URL: <https://doi.org/10.1016/j.ces.2007.11.016>

Husain Khan, A., Abdul Aziz, H., Palaniandy, P., Naushad, M., Cevik, E. and Zahmatkesh, S. (2023), 'Pharmaceutical residues in the ecosystem: Antibiotic resistance, health impacts, and removal techniques', *Chemosphere* **339**, 139647.

URL: <https://doi.org/10.1016/j.chemosphere.2023.139647>

Islam, M. A., Nazal, M., Sajid, M. and Suliman, M. A. (2024), 'Adsorptive removal of paracetamol from aqueous media: A review of adsorbent materials, adsorption mechanisms, advancements, and future perspectives', *Journal of Molecular Liquids* **396**, 123976.

URL: <https://doi.org/10.1016/j.molliq.2024.123976>

Koagouw, W., Arifin, Z., Olivier, G. and Ciocan, C. (2021), 'High concentrations of paracetamol in effluent dominated waters of jakarta bay, indonesia', *Marine Pollution Bulletin* **169**, 112558.

URL: <https://doi.org/10.1016/j.marpolbul.2021.112558>

Kuttiani Ali, J., Abi Jaoude, M. and Alhseinat, E. (2021), 'Polyimide ultrafiltration membrane embedded with reline-functionalized nanosilica for the remediation of pharmaceuticals in water', *Separation and Purification Technology* **266**, 118585.

URL: <https://doi.org/10.1016/j.seppur.2021.118585>

Li, Y., Gong, X., Sun, Y., Shu, Y., Niu, D. and Ye, H. (2022), 'High molecular weight fractions of dissolved organic matter (dom) determined the adsorption and electron transfer capacity of dom on iron minerals', *Chemical Geology* **604**, 120907.

URL: <https://doi.org/10.1016/j.chemgeo.2022.120907>

MacKeown, H., Benedetti, B., Scapuzzi, C., Di Carro, M. and Magi, E. (2022), 'A review on polyethersulfone membranes in polar organic chemical integrative samplers: Preparation, characterization and innovation', *Critical Reviews in Analytical Chemistry* pp. 1–17.

URL: <https://doi.org/10.1080/10408347.2022.2131374>

Mirzaei, A., Chen, Z., Haghghat, F. and Yerushalmi, L. (2017), 'Removal of pharmaceuticals from water by

homo/heterogenous fenton-type processes – a review', *Chemosphere* **174**, 665–688.

URL: <https://doi.org/10.1016/j.chemosphere.2017.02.019>

Nandiyanto, A., Oktiani, R. and Ragadhita, R. (2019), 'How to read and interpret ftir spectroscopy of organic material', *Indonesian Journal of Science and Technology* **4**(1), 97.

URL: <https://doi.org/10.17509/ijost.v4i1.15806>

Pacheco-Álvarez, M., Picos Benítez, R., Rodríguez-Narváez, O., Brillas, E. and Peralta-Hernández, J. (2022), 'A critical review on paracetamol removal from different aqueous matrices by fenton and fenton-based processes, and their combined methods', *Chemosphere* .

URL: <https://doi.org/10.1016/j.chemosphere.2022.134883>

Phong Vo, H., Le, G., Hong Nguyen, T., Bui, X.-T., Nguyen, K., Rene, E., Vo, T., Thanh Cao, N.-D. and Mohan, R. (2019), 'Acetaminophen micropollutant: Historical and current occurrences, toxicity, removal strategies and transformation pathways in different environments', *Chemosphere* **236**, 124391.

URL: <https://doi.org/10.1016/j.chemosphere.2019.124391>

Rosman, N., Salleh, W., Mohamed, M., Jaafar, J., Ismail, A. and Harun, Z. (2018), 'Hybrid membrane filtration-advanced oxidation processes for removal of pharmaceutical residue', *Journal of Colloid and Interface Science* **532**, 236–260.

URL: <https://doi.org/10.1016/j.jcis.2018.07.118>

Sychev, A. and Isak, V. (1995), 'Iron compounds and the mechanisms of the homogeneous catalysis of the activation of o₂ and h₂o₂ and of the oxidation of organic substrates', *Russian Chemical Reviews* **64**(12), 1105–1129.

URL: <https://doi.org/10.1070/RC1995v064n12ABEH000195>

Van, H., Nguyen, L., Hoang, T., Nguyen, T., Tran, T., Nguyen, T., Vu, X., Pham, M., Tran, T., Pham, T. et al. (2020), 'Heterogeneous fenton oxidation of paracetamol in aqueous solution using iron slag as a catalyst: Degradation mechanisms and kinetics', *Environmental Technology & Innovation* **18**, 100670.

URL: <https://doi.org/10.1016/j.eti.2020.100670>

Ziembowicz, S. and Kida, M. (2022), 'Limitations and future directions of application of the fenton-like process in micropollutants degradation in water and wastewater treatment: A critical review', *Chemosphere* **296**, 134041.

URL: <https://doi.org/10.1016/j.chemosphere.2022.134041>